

Instantons and scalar multiquark states: From small to large N_c

T. Schäfer

*Department of Physics, North Carolina State University, Raleigh, North Carolina 17695, USA
and Riken-BNL Research Center, Brookhaven National Laboratory, Upton, New York 11973, USA*

(Received 25 September 2003; published 30 December 2003)

We study scalar $(\bar{q}q)$ and $(\bar{q}q)^2$ correlation functions in the instanton liquid model. We show that the instanton liquid supports a light scalar-isoscalar (sigma) meson, and that this state is strongly coupled to both $(\bar{q}q)$ and $(\bar{q}q)^2$. The scalar-isovector a_0 meson, on the other hand, is heavy. We also show that these properties are specific to QCD with three colors. In the large N_c limit the scalar-isoscalar meson is not light, and it is mainly coupled to $(\bar{q}q)$.

DOI: 10.1103/PhysRevD.68.114017

PACS number(s): 12.38.Lg, 11.15.Pg, 13.75.Lb

I. INTRODUCTION

There is a long-standing controversy concerning the structure of scalar-isoscalar mesons in QCD [1–9]. One view is that scalar mesons are p -wave $q\bar{q}$ bound states with masses in the 1.0–1.5-GeV range. According to this view the large effects seen in the $I=0$ $\pi\pi$ and $I=1/2$ πK channel are due to t -channel meson exchanges and other coupled channel effects. The competing view is that there are genuine scalar resonances below 1 GeV, and that the structure of these states is quite different from ordinary quark model $q\bar{q}$ states.

Jaffe suggested that the unusual properties of the light scalar mesons could be explained by assuming a large $(qq)(\bar{q}\bar{q})$ admixture [2,7]. He observed that the spectrum of the flavor nonet obtained by coupling two antitriplet scalar diquarks is inverted as compared to a standard $q\bar{q}$ nonet, and contains a light isospin singlet, a strange doublet, and a heavy triplet plus singlet with hidden strangeness. This compares very favorably to the observed light sigma, the strange kappa, and the heavier $a_0(980)$ and $f_0(980)$. It also explains why the a_0 and f_0 are strongly coupled to $K\bar{K}$ and $\pi\eta$. Strong correlations in the antitriplet scalar diquark channel are quite natural in QCD and have also been invoked in order to understand the structure of baryons [10,11] and dense baryonic matter [12,13].

In this work we study the nature of scalar-isoscalar mesons in the instanton model [14,15]. There are several reasons why instantons effects are relevant. Scalar-isoscalar mesons have vacuum quantum numbers and are directly related to fluctuations in the chiral condensate. There is an impressive amount of evidence from lattice calculations that instantons are responsible for chiral symmetry breaking in QCD [16–18]. These calculations also suggest that the approximate zero modes responsible for chiral symmetry breaking are small in size. This implies that the chiral condensate is very inhomogeneous and that fluctuations in the scalar channel are large. In addition to that, if there is a large $(qq)(\bar{q}\bar{q})$ admixture in the wave function of scalar mesons, both flavor mixing and off-diagonal $(q\bar{q})$ – $(q\bar{q})^2$ mixing have to be large. The instanton induced $(q\bar{q})^{N_f}$ interaction provides a natural mechanism for these effects.

In order to study the nature of scalar-isoscalar mesons we

compute both $(q\bar{q})$ and $(qq)(\bar{q}\bar{q})$ correlation functions. We show that there is a large scalar resonance signal in both the diagonal $(q\bar{q})$ and $(qq)(\bar{q}\bar{q})$ correlators as well as the off-diagonal $(q\bar{q})$ – $(qq)(\bar{q}\bar{q})$ correlator. This implies that there is indeed a large four quark admixture in the scalar-isoscalar meson. We have to note, however, that in a relativistic quantum field theory this statement is somewhat hard to quantify. We can compute the coupling of the $(q\bar{q})$ and $(qq)(\bar{q}\bar{q})$ operators to the scalar resonance, but these coupling constants have different dimensions and it is not clear how to compare them.

We address this problem by studying scalar correlators for different numbers of colors. We expect that in the large N_c limit the scalar meson becomes a “normal” quark model state which is dominated by the $(q\bar{q})$ component. This implies that there is no scalar resonance signal in the four quark channel, and that the scalar-isoscalar and scalar-isovector correlators become indistinguishable. We show that this tendency is clearly seen in ratios of correlation functions computed in QCD with different numbers of colors.

This paper is organized as follows. In Sec. II we define $(q\bar{q})$ and $(qq)(\bar{q}\bar{q})$ scalar correlation functions. In Sec. III we discuss the short distance behavior of these correlators and investigate the importance of unphysical contributions in the quenched approximation. In Sec. IV we present numerical results from quenched and unquenched simulations of the instanton liquid model.

II. SCALAR CORRELATORS

The lowest dimension operator with the quantum numbers of the sigma meson is the scalar $(q\bar{q})$ operator

$$j_{(q\bar{q})} = \frac{1}{\sqrt{2}}(\bar{u}u + \bar{d}d). \quad (1)$$

The corresponding correlation function is (see Fig. 1)

$$\begin{aligned} \Pi_{(q\bar{q})}(x) &= \mathcal{O}(x) - 2T(x) \\ &= \langle \text{Tr}[S(0,x)S(x,0)] \rangle \\ &\quad - 2\langle \text{Tr}[S(0,0)]\text{Tr}[S(x,x)] \rangle, \end{aligned} \quad (2)$$

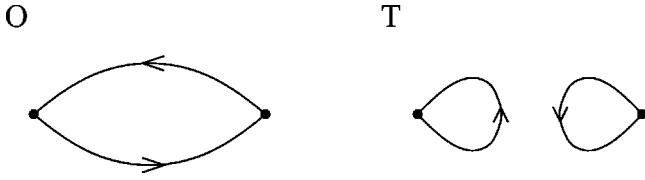


FIG. 1. Quark line diagrams contributing to the scalar ($q\bar{q}$) correlation function, (O) “one-loop,” and (T) “two-loop.” The lines are quark propagators in a gluonic background field.

where $\langle \cdot \rangle$ is an average over all gluonic field configurations, $S(0,x)$ is the full quark propagator in a given background gluonic field, and the trace is taken over Dirac and color indices. $O(x)$ and $T(x)$ denote the one-loop (connected) and two-loop (disconnected) terms in the correlation function. Note that the quark line connected term is equal to the correlator of the scalar-isovector current, $\Pi_{a_0}(x) = O(x)$. Lattice calculations of the correlation function (2) have been reported in Refs. [19–22].

There are several ways to construct scalar-isoscalar four quark operators. One possibility is to couple two quark-antiquark operators. We expect the most attractive channel to arise from the coupling of two color-singlet, flavor-triplet pseudoscalar operators,

$$j_{(q\bar{q})^2} = (\bar{q} \gamma_5 \tau^a q)(\bar{q} \gamma_5 \tau^a q). \quad (3)$$

The corresponding correlation function is equal to the $I=0$ two-pion correlator [23]

$$\begin{aligned} \Pi_{I0}(x) &= \frac{1}{4!} \langle j_{(q\bar{q})^2}(0) j_{(q\bar{q})^2}(x) \rangle \\ &= D(x) + \frac{1}{2} C(x) - 3A(x) + \frac{3}{2} G(x), \end{aligned} \quad (4)$$

where

$$D(x) = \langle (\text{Tr}[S(0,x) \gamma_5 S(x,0) \gamma_5])^2 \rangle \quad (5)$$

$$C(x) = \langle \text{Tr}[S(0,x) \gamma_5 S(x,0) \gamma_5]^2 \rangle \quad (6)$$

$$A(x) = \langle \text{Tr}[S(0,x) \gamma_5 S(x,x) \gamma_5 S(x,0) \gamma_5 S(0,0) \gamma_5] \rangle \quad (7)$$

$$G(x) = \langle \text{Tr}[(S(0,0) \gamma_5)^2] \text{Tr}[(S(x,x) \gamma_5)^2] \rangle \quad (8)$$

are the four quark correlators shown in Fig. 2. The $I=2$ two-pion correlator is given by

$$\Pi_{I2}(x) = D(x) - C(x) \quad (9)$$

and does not involve any disconnected diagrams. The mixed $(q\bar{q})-(q\bar{q})^2$ correlation function is given by (see Fig. 3)

$$\begin{aligned} \Pi_{(q\bar{q})-I0}(x) &= \frac{1}{3!} \langle j_{(q\bar{q})}(0) j_{(q\bar{q})^2}(x) \rangle \\ &= \sqrt{2}(A_{\text{mix}}(x) - G_{\text{mix}}(x)), \end{aligned} \quad (10)$$

where

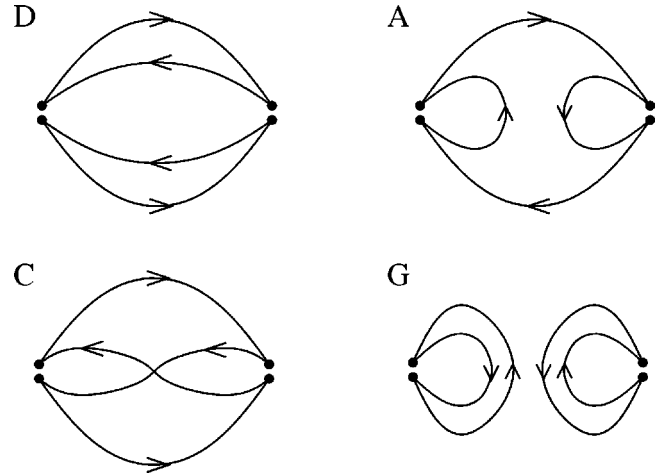


FIG. 2. Quark line diagrams contributing to the two-pion correlation function, (D) “direct,” (C) “crossed,” (A) “single annihilation,” and (G) “double annihilation” or “glue.”

$$A_{\text{mix}}(x) = \langle \text{Tr}[S(0,x) \gamma_5 S(x,x) \gamma_5 S(x,0)] \rangle \quad (11)$$

$$G_{\text{mix}}(x) = \langle \text{Tr}[S(0,0)] \text{Tr}[(S(x,x) \gamma_5)^2] \rangle. \quad (12)$$

Instead of coupling two quark-antiquark operators we can construct scalar-isoscalar four quark operators by coupling a diquark and an antidiquark operator. The most attractive channel is expected to arise from two color antitriplet and isospin singlet scalar diquarks

$$j_{(d\bar{q})^2} = \epsilon^{abc} \epsilon^{ade} (q^b C \gamma_5 \tau_2 q^c) (\bar{q}^d C \gamma_5 \tau_2 \bar{q}^e). \quad (13)$$

This operator can be Fierz rearranged into a $(q\bar{q})^2$ operator. The result is

$$\begin{aligned} j_{(d\bar{q})^2} &= \frac{1}{4} \left\{ (\bar{q} \gamma_5 \bar{\tau}^a q) (\bar{q} \gamma_5 \bar{\tau}^a q) + (\bar{q} \bar{\tau}^a q) (\bar{q} \bar{\tau}^a q) \right. \\ &\quad + (\bar{q} \gamma_\mu \bar{\tau}^a q) (\bar{q} \gamma_\mu \bar{\tau}^a q) + (\bar{q} \gamma_5 \gamma_\mu \bar{\tau}^a q) (\bar{q} \gamma_5 \gamma_\mu \bar{\tau}^a q) \\ &\quad \left. - \frac{1}{2} (\bar{q} \sigma_{\mu\nu} \bar{\tau}^a q) (\bar{q} \sigma_{\mu\nu} \bar{\tau}^a q) \right\} \end{aligned} \quad (14)$$

where $\bar{\tau}^a = (\vec{\tau}, i)$. Note that the flavor structure of Eq. (14) is that of a determinant, $(\bar{q} \bar{\tau}^a q) (\bar{q} \bar{\tau}^a q) = (\bar{u}u)(\bar{d}d)$

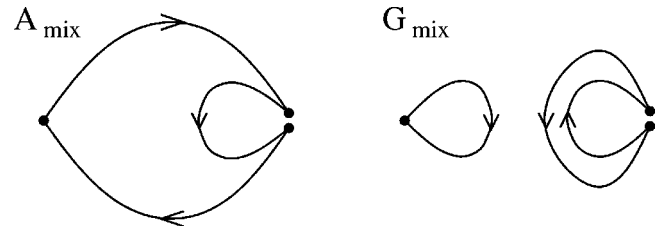


FIG. 3. Quark line diagrams contributing to the off-diagonal scalar two-pion correlation function, (A_{mix}) “single annihilation,” and (G_{mix}) “double annihilation” or “glue.”

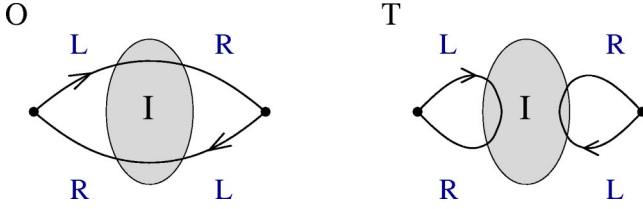


FIG. 4. Single instanton contributions to the scalar correlation function. The lines crossing the shaded area correspond to zero mode propagators, and L and R label the chirality of the quark. The anti-instanton contribution corresponds to $L \leftrightarrow R$.

$-(\bar{u}d)(\bar{d}u)$. Equation (14) contains both attractive channels, such as $\pi\pi$ and f_0f_0 , as well as repulsive channels, such as $\eta'\eta'$ and a_0a_0 . In the following we will concentrate on the $\pi\pi$ channel equation (3).

III. SCALAR CORRELATORS IN THE INSTANTON MODEL

In this section we wish to study instanton contributions to the scalar correlation functions (2), (4), and (9) and Eq. (10). At short distances only the effect of the closest instanton has to be taken into account. The main instanton contribution is related to the zero mode term in the fermion propagator

$$S(x, y) \approx \frac{\psi_0(x-z)\psi_0^\dagger(y-z)}{m^*}, \quad (15)$$

where $\psi_0(x)$ is the zero mode wave function and z is the location of the instanton. For an isolated instanton $m^* = m_q$ where m_q is the current quark mass. In an ensemble of instantons m^* is an effective mass $m^* \simeq \pi\rho(2/N_c)^{1/2}(N/V)^{1/2}$. Here, ρ is the average instanton size and N/V is the average instanton density. Instanton zero modes make equal contributions to the one and two-loop terms in the scalar correlation function (2), $O_{inst} = T_{inst} < 0$, see Fig. 4. As a consequence the one-instanton contribution is attractive in the σ channel and repulsive in the a_0 channel. Averaging over the position of the instanton we get

$$\begin{aligned} \Pi_{\sigma, a_0}^{SIA}(x) = \pm \int d\rho n(\rho) \frac{6\rho^4}{\pi^2} \frac{1}{(m^*)^2} \frac{\partial^2}{\partial(x^2)^2} \\ \times \left\{ \frac{4\xi^2}{x^4} \left(\frac{\xi^2}{1-\xi^2} + \frac{\xi}{2} \log \frac{1+\xi}{1-\xi} \right) \right\}, \quad (16) \end{aligned}$$

where $n(\rho)$ is the instanton size distribution and $\xi^2 = x^2/(x^2 + 4\rho^2)$. The one-instanton contribution can be resummed using the random phase approximation (RPA) [24–26]

$$\Pi_{\sigma, a_0}^{RPA}(x) = N_c \left(\frac{N_c V}{N} \right) \int d^4 q e^{iq \cdot x} \Gamma_s(q) \frac{\pm 1}{1 \pm C_s(q)} \Gamma_s(q). \quad (17)$$

The loop and vertex functions C_s and Γ_s are given by

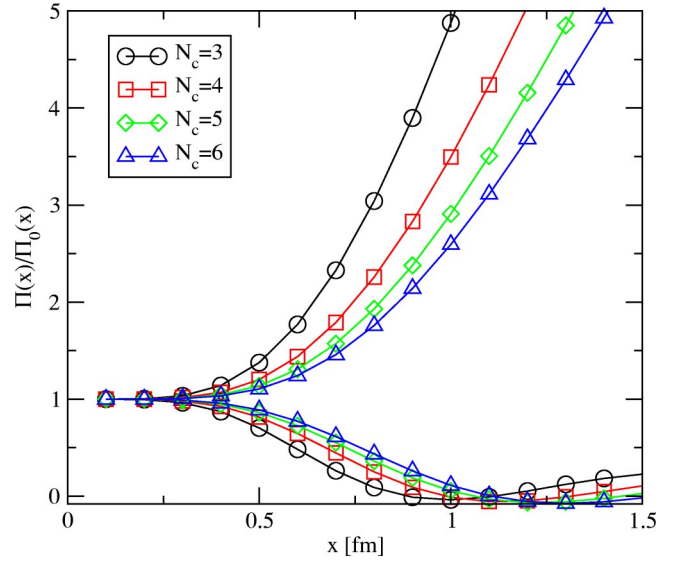


FIG. 5. Scalar-isoscalar (σ) and scalar-isovector (a_0) correlation functions for different numbers of colors N_c calculated in the random phase approximations approximation to the instanton liquid model. The correlation functions are normalized to free field behavior $\Pi_0(x) \sim 1/x^6$. The upper/lower curves correspond to the σ/a_0 , respectively.

$$C_s(q) = 4N_c \left(\frac{V}{N} \right) \int \frac{d^4 p}{(2\pi)^4} \frac{M_1 M_2 (M_1 M_2 - p_1 \cdot p_2)}{(M_1^2 + p_1^2)(M_2^2 + p_2^2)}, \quad (18)$$

$$\Gamma_s(q) = 4 \int \frac{d^4 p}{(2\pi)^4} \frac{(M_1 M_2)^{1/2} (M_1 M_2 - p_1 \cdot p_2)}{(M_1^2 + p_1^2)(M_2^2 + p_2^2)}, \quad (19)$$

where $p_1 = p + q/2$, $p_2 = p - q/2$ and $M_{1,2} = M(p_{1,2})$ are momentum dependent effective quark masses. In the instanton liquid model the momentum dependence of the effective quark mass is governed by the Fourier transform of the instanton zero mode profile. The effective quark mass at zero virtuality, $M(0)$, is determined by a Dyson-Schwinger equation. For typical values of the parameters $\rho \simeq 0.3$ fm and $(N/V) = 1$ fm $^{-4}$ we find $M(0) \simeq 350$ MeV.

Scalar correlation functions in the RPA approximation are shown in Fig. 5. We observe that the isoscalar and isovector correlation functions are indeed very different. We also note that the isovector correlator is unphysical for $x > 0.7$ fm. This is an artifact of the quenched approximation and can be understood in terms of quenched $\pi\eta'$ intermediate states. The quenched σ correlation function receives unphysical $\eta'\eta'$ contributions, but these terms are not included in the random phase approximation. The scalar-isoscalar (σ) correlator shows a clear resonance signal. A simple pole fit gives $m_\sigma = 540$ MeV. We observe that the σ and a_0 correlation functions become more similar as the number of colors increases. However, in the RPA approximation the difference remains finite and large in the limit $N_c \rightarrow \infty$. As explained in Ref. [27] this is related to a failure of the RPA approximation when applied to the large N_c instanton liquid.

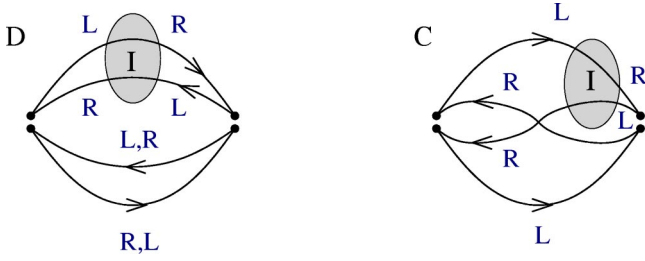


FIG. 6. Instantons contributions to the $\pi\pi$ correlation functions. At the one-instanton level, there are no contributions to the single and double annihilation diagrams.

Let us now study instanton contributions to the two-pion correlation functions (4) and (9). The first possibility is that all four quarks propagate in zero mode states. In QCD with $N_f=2,3$ flavors this contribution violates the Pauli principle and has to vanish. This is reflected by the fact that in both the $I=0$ and 2 correlation functions the sum of the coefficients of the four different contractions, D , C , A and G , vanishes. We note that for light quark masses it is dangerous to drop the disconnected contributions to the $I=0$ correlator, an approximation sometimes referred to as the quenched valence approximation. In particular, there is a large positive zero mode contribution to the connected $I=0$ correlation function which is not present in the full $I=0$ correlator.

Contributions with an odd number of fermion zero modes violate chirality. This leaves terms with two zero mode propagators, see Fig. 6. These terms only appear in the direct and crossed diagrams. The one-instanton contribution to the direct diagram is $D^{SIA}(x) = 2\Pi_\pi^0(x)\Pi_\pi^{SIA}(x)$, where $\Pi_\pi^0(x) = 3/(\pi^4 x^6)$ is the free quark contribution and $\Pi_\pi^{SIA}(x) = \Pi_\sigma^{SIA}(x)$ is the single instanton contribution to the pion correlation function. It is clear that $D^{SIA}(x)$ simply corresponds to two non-interacting pions. Interactions arise from the crossed term. We find

$$\Pi_{I0}^{SIA}(x) = 2\Pi_\pi^0(x)\Pi_\pi^{SIA}(x) + \frac{1}{6}\Pi_\pi^0(x)\Pi_\pi^{SIA}(x) \quad (20)$$

$$\Pi_{I2}^{SIA}(x) = 2\Pi_\pi^0(x)\Pi_\pi^{SIA}(x) - \frac{1}{3}\Pi_\pi^0(x)\Pi_\pi^{SIA}(x). \quad (21)$$

This implies that the one-instanton term is attractive in the $I=0$ channel and repulsive in the $I=2$ channel. One can try to resum this interaction in order to study the $\pi\pi$ interaction at intermediate and long distances. For the one-gluon exchange interaction, this problem was recently studied in Ref. [28]. At very low momenta, the $\pi\pi$ interaction is constrained by chiral symmetry. Weinberg predicted the s -wave scattering lengths in the $I=0$ and $I=2$ channels [29]

$$a_0^0 = \frac{7m_\pi}{32\pi f_\pi^2}, \quad a_0^2 = -\frac{m_\pi}{16\pi f_\pi^2}. \quad (22)$$

We emphasize, however, that our objective in this work is not a determination of the scattering lengths, but a study of scalar resonances. In Sec. IV we will describe how to sum

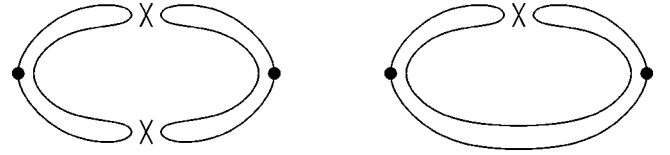


FIG. 7. Diagrams that lead to quenching artifacts in the two-pion correlation function. The diagram on the left and right show the two and one double-hairpin terms.

the instanton induced interaction to all orders by performing numerical simulations of the $I=0,2$ $\pi\pi$ correlation functions in the instanton model.

At the one-instanton level there is no contribution to the mixed $(q\bar{q})-(q\bar{q})^2$ correlation function. This is a consequence of the fact that in $N_f=2$ QCD not all quarks can propagate in zero mode states. In QCD with three flavors there is a flavor mixing $(\bar{u}u)(\bar{d}d)(\bar{s}s)$ contribution.

Finally, we have to understand the effect of the quenched approximation on the isoscalar two-pion correlation function [30,31]; see Fig. 7. The main artifact in the quenched approximation arises from unphysical $\eta'\eta'$ intermediate states. The long distance, low momentum part of the quenched η' propagator is of the form

$$\Pi_{\eta'}(q) = \frac{\lambda_\pi^2}{q^2 + m_\pi^2} - \frac{\lambda_\pi^2}{q^2 + m_\pi^2} m_0^2 \frac{1}{q^2 + m_\pi^2}, \quad (23)$$

where the second term is the so-called double-hairpin contribution, $m_0^2 \approx m_{\eta'}^2$, is related to the η' mass and λ_π is the coupling of the pion to the pseudoscalar current. Note that the double hairpin term is negative in euclidean space. Using Eq. (23) we see that the $\eta'\eta'$ contribution to the $I=0$ $\pi\pi$ correlation function contains a one double-hairpin term which is negative and a two double-hairpin term which is positive in euclidean space. Numerical results for the coordinate space correlation function are shown in Fig. 8. The correlation function is normalized to the square of the pion correlator. For comparison we also show the contribution of a scalar σ resonance with mass $m_\sigma = 500$ MeV and coupling constant $\lambda_\sigma = (350 \text{ MeV})^5$. We observe that the quenched approximation leads to unphysical contributions that are repulsive at intermediate distances $x \sim 0.5$ fm and large and attractive at large distance. We also observe that these effects will mask the presence of a sigma resonance, unless the sigma coupling is very large.

IV. NUMERICAL RESULTS

In this section we present numerical results obtained in quenched and unquenched simulations of the instanton liquid model [32,33]. The main assumption of the instanton liquid model is that the QCD partition function

$$Z = \int DA_\mu \exp(-S) \prod_f^{N_f} \det(i\mathcal{D} + im_f) \quad (24)$$

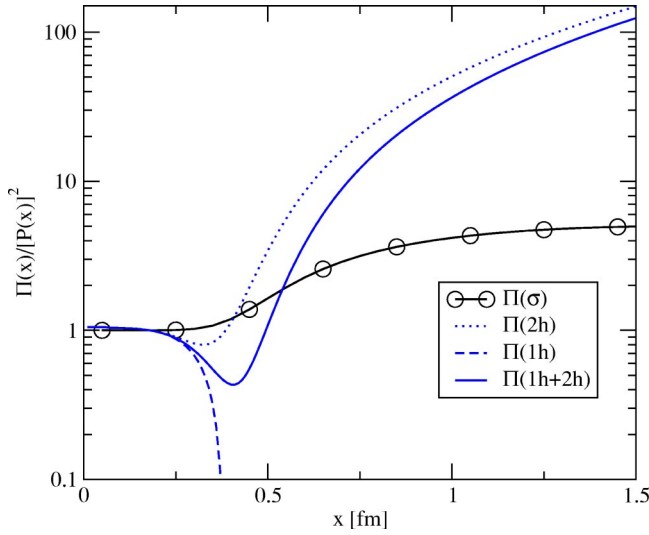


FIG. 8. Quenched $\eta' \eta'$ contribution to the $I=0$ $\pi\pi$ correlation function normalized to the square of the pion correlation function. The curves labeled (1h) and (2h) show the one and two double-hairpin diagram; see Fig. 7. For comparison, we also show the contribution of a scalar resonance.

is dominated by classical gauge configurations called instantons. Instantons in QCD with N_c colors are characterized by $4N_c$ collective coordinates, position (4), size (1), and color orientation ($4N_c-5$). An ensemble of instantons is governed by the partition function

$$Z = \sum_{N_I, N_A} \frac{1}{N_I N_A} \int \prod_i^{N_I + N_A} [d\Omega_i d(\rho_i)] \times \exp(-S) \prod_f^{N_f} \det(i\mathcal{D} + im_f), \quad (25)$$

where $\Omega = (z_i, \rho_i, U_i)$ labels the collective coordinates and $d(\rho)$ is the instanton measure. Correlation functions are computed from the quark propagator in a given instanton configuration. The propagator is determined by numerically inverting the Dirac operator in the space of approximate zero modes. The short distance part is added perturbatively.

Most of the results presented below were obtained from simulations at a quark mass $m_q = 20$ MeV in a Euclidean box with dimensions $(2.83 \text{ fm})^3 \times 5.66 \text{ fm}$. We have not systematically studied finite volume corrections. Finite volume effects on the two-pion correlator can be used in order to determine pion scattering lengths [34]. Our aim in this work is not a determination of the $\pi\pi$ scattering length, but a study of $\pi\pi$ resonances.

Scalar-isoscalar and scalar-isovector correlation functions are shown in Fig. 9. We note that the scalar-isoscalar σ and scalar-isovector a_0 correlators behave very differently. The a_0 correlator is very repulsive. In the quenched approximation the correlation function even becomes negative. This behavior can be understood in terms of quenched $\eta' \pi$ intermediate states. In full QCD the correlator is still quite repulsive. We extract a resonance mass $m_{a_0} \sim 1$ GeV. The sigma

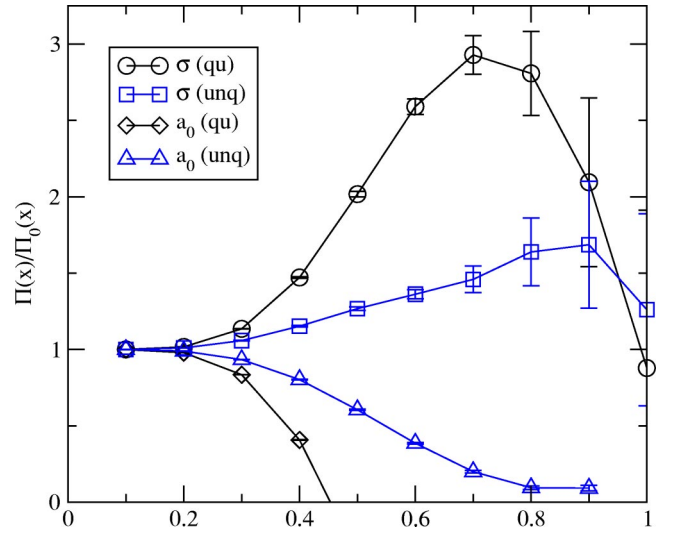


FIG. 9. Scalar-isoscalar σ and scalar-isovector a_0 correlation functions in the instanton model. The correlators are normalized to free field behavior $\Pi_0(x) \sim 1/x^6$. The labels (qu) and (unq) refer to the quenched and unquenched correlation functions.

correlator, on the other hand, is very attractive, both in quenched and full QCD. Because of the large vacuum contribution $\langle (\bar{q}q)^2 \rangle$ it is hard to extract the mass. Our results are consistent with a light scalar $m_\sigma = (0.55-0.70)$ GeV.

In Fig. 10 we show $I=0, 2$ $\pi\pi$ correlation functions in the quenched approximation. The results are normalized to the square of the pion correlation function. We observe that the $I=2$ $\pi\pi$ correlator is indeed repulsive, the correlation function is suppressed as compared to the square of the pion correlator. The connected part of the $I=0$ correlator is very strongly enhanced and has an unusual shape. This is due to

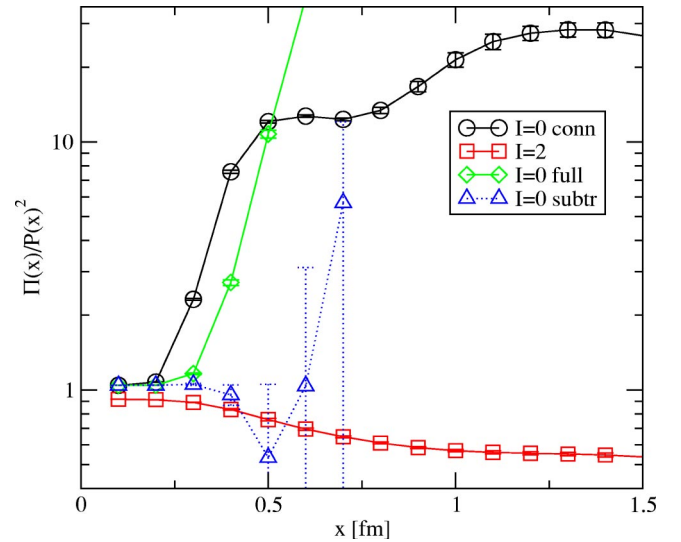


FIG. 10. $I=0$ and 2 two-pion correlation functions measured in quenched simulations of the instanton liquid model. The correlators are normalized to the square of the pion correlation function. The curve labeled (conn) shows the connected part of the $I=0$ correlator (full) is the complete $I=0$ correlator, and (subtr) is the complete correlator after the vacuum contribution is subtracted.

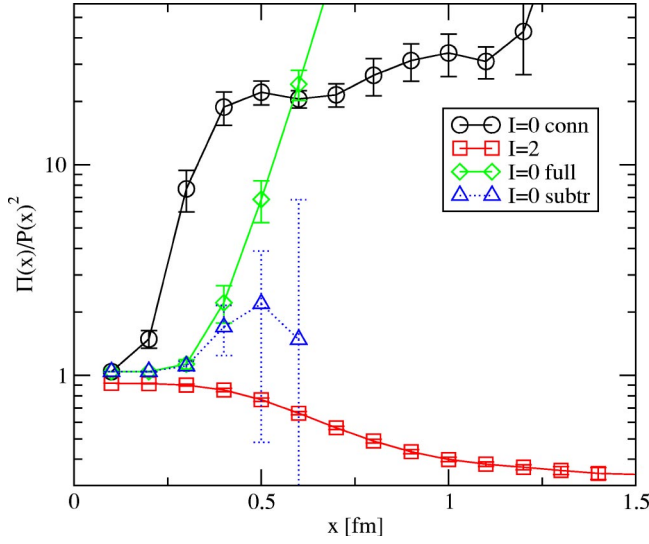


FIG. 11. $I=0$ and 2 two-pion correlation functions measured in unquenched simulations of the instanton liquid model. Curves labeled as in Fig. 10.

the effect discussed in Sec. III. The connected $I=0$ correlator receives a large Pauli principle violating zero mode contribution. The full $I=0$ correlator has a vacuum contribution $\langle(\bar{q}\tau^a q)^2\rangle^2$ that needs to be subtracted. The subtraction involves large cancellations and the result has large statistical uncertainties for $x > 0.5$ fm. We note that the subtracted correlation function is repulsive at intermediate distances $x \sim 0.5$ fm. As explained in Sec. III this is an artifact of the quenched approximation.

Unquenched $\pi\pi$ correlation functions are shown in Fig. 11. We observe that the $I=2$ correlation function is not strongly modified as compared to the unquenched calculation. The same is true for the connected $I=0$ correlator. However, the full (subtracted) $I=0$ correlator is strongly modified. The correlation function is now attractive at intermediate distances $x \sim 0.5$ fm. The data are not sufficiently accurate to determine the mass of a resonance, but the resonance parameters can be estimated if the data are combined with the diagonal $(q\bar{q})$ and off-diagonal $(q\bar{q})-(q\bar{q})^2$ correlators. We find $m_\sigma = 600$ MeV and $\lambda_\sigma = (330 \text{ MeV})^5$.

In Figs. 12–14 we show the behavior of the correlation functions for different numbers of colors $N_c = 3, \dots, 6$ [27]. We find that the difference between the scalar-isoscalar and scalar-isovector correlation functions disappears as the number of colors increases. For $N_c = 6$ the mass of the sigma is $m_\sigma > 1$ GeV. The physical reason for the change in the sigma meson correlation function is the fact that the chiral condensate becomes more homogeneous as the number of colors increases. The main change in the scalar-isovector correlation function is the disappearance of quenched $\eta'\pi$ intermediate states. We expect that the unquenched a_0 mass is fairly independent of the number of colors.

Figure 13 shows that the off-diagonal $(q\bar{q})-(q\bar{q})^2$ correlation function decreases dramatically as the number of colors increases. The results are consistent with the idea that the off-diagonal correlation function vanishes in the large N_c

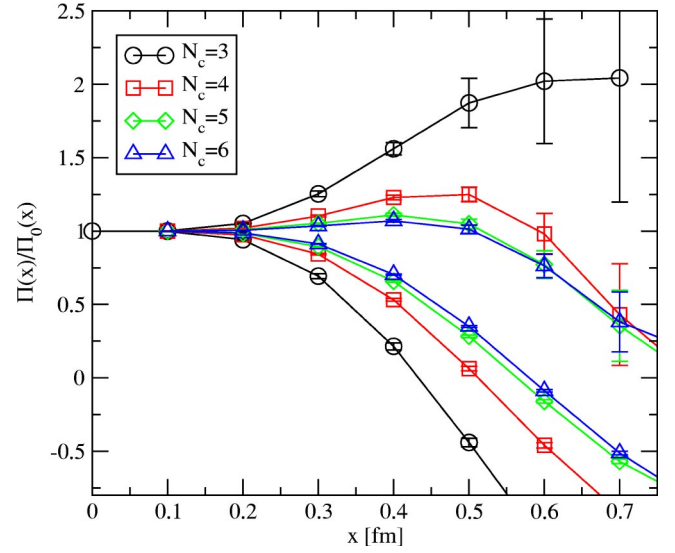


FIG. 12. Scalar-isoscalar (σ) and scalar-isovector (a_0) correlation functions for different numbers of colors N_c . The correlators are normalized to free field behavior, $\Pi^0(x) \sim N_c/x^6$. The upper/lower curves correspond to the σ/a_0 , respectively. The data shown in this figure were obtained from quenched simulations of the instanton liquid model.

limit. The $I=2$ $\pi\pi$ correlator is only weakly affected by the number of colors. We observe, however, that the $I=2$ correlation function tends towards the noninteracting $\pi\pi$ correlator. The connected $I=0$ correlator, on the other hand, shows a very dramatic decrease towards the non-interaction two pion correlation function as the number of colors increases.

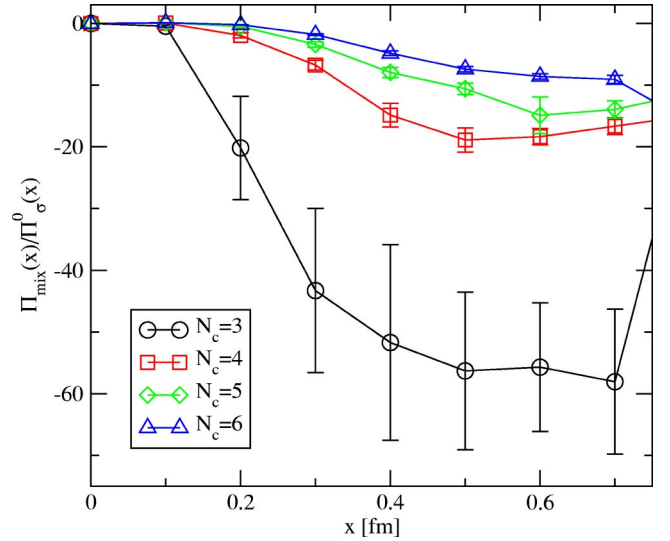


FIG. 13. Off-diagonal $(q\bar{q})-(q\bar{q})^2$ correlation function for different values of the numbers of colors N_c . The correlation functions are normalized to the free $(q\bar{q})$ correlator. The data shown in this figure were obtained from quenched simulations of the instanton liquid model.

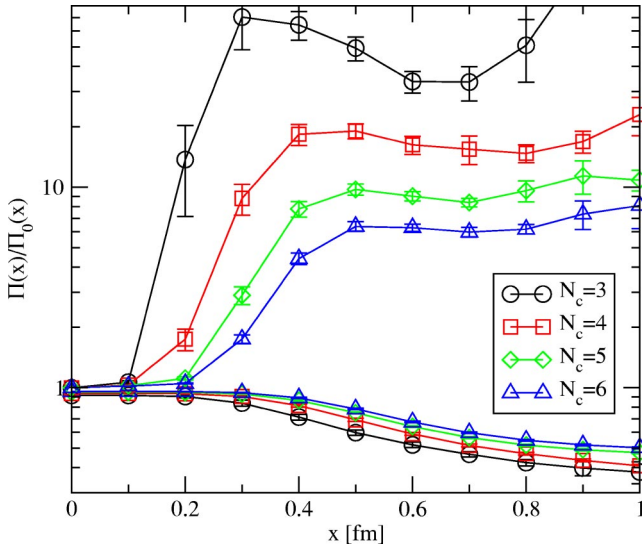


FIG. 14. Connected $I=0$ and $I=2$ two-pion correlation functions for different values of the numbers of colors N_c .

V. SUMMARY

In this paper we studied scalar $(q\bar{q})$ and $(q\bar{q})^2$ correlation functions in the instanton model. We showed that the structure of the scalar-isoscalar σ and scalar-isovector a_0 mesons is very different. The correlation function in the a_0 channel is very repulsive while the σ channel is strongly attractive. The scalar $(q\bar{q})$ correlator is consistent with a light sigma resonance with a mass $m_\sigma = (550 - 700)$ MeV [9,26,32,33]. A light sigma resonance also appears in Nambu-Jona-Lasinio models [35]. However, the large OZI violation in the scalar channel is characteristic of the instanton induced interaction.

We also showed that the sigma couples strongly to the $I = 0$ $(q\bar{q})^2$ current. Observing this effect not only requires a calculation of both the connected and disconnected dia-

grams, but also the inclusion of the fermion determinant. If the calculation is restricted to connected diagrams, or performed in the quenched approximation, the scalar resonance is masked by large unphysical contributions.

We showed that the special properties of the sigma meson, its small mass and large coupling to $(q\bar{q})^2$ states, are specific to QCD with three colors. If the number of colors is increased the sigma becomes an “ordinary” meson with a mass in the 1 GeV range and small coupling to $(q\bar{q})^2$ states. The physical reason is that the chiral condensate is very inhomogeneous in $N_c=3$ QCD, but becomes more homogeneous as the number of colors increases. The large inhomogeneity of the condensate in $N_c=3$ QCD reflects the small size of the instanton. The chiral condensate becomes more homogeneous as N_c grows because the instanton liquid is more dense. As emphasized in Ref. [27] this does not necessarily imply that instantons overlap strongly, since the instanton density grows like the volume of the color group.

There are many interesting problems that remain to be studied. In this paper we concentrated on scalar mesons in $N_f=2$ flavor QCD. One of the remarkable aspects of $(qq)(\bar{q}\bar{q})$ states in $N_f=3$ QCD is their flavor structure. In particular, one would like to verify that there is hidden strangeness in the heavy scalars. In addition to the meson-meson or diquark-antidiquark interaction we would also like to study diquark-diquark correlations. This problem is relevant to the structure of dense baryonic matter [36], the spectrum of $(qq)^2\bar{q}$ pentaquark states [37], and the possible existence of the H dibaryon [38].

ACKNOWLEDGMENTS

We would like to thank E. Shuryak for useful discussions. This work was supported in part by U.S. DOE Grant No. DE-FG02-03ER41260.

-
- [1] S. Spanier and N.A. Tornqvist, in Particle Data Group, K. Hagiwara *et al.*, Phys. Rev. D **66**, 010001 (2002).
 - [2] R.L. Jaffe, Phys. Rev. D **15**, 267 (1977).
 - [3] J.D. Weinstein and N. Isgur, Phys. Rev. Lett. **48**, 659 (1982).
 - [4] D. Lohse, J.W. Durso, K. Holinde, and J. Speth, Nucl. Phys. **A516**, 513 (1990).
 - [5] N.A. Tornqvist and M. Roos, Phys. Rev. Lett. **76**, 1575 (1996).
 - [6] D. Black, A.H. Fariborz, F. Sannino, and J. Schechter, Phys. Rev. D **59**, 074026 (1999).
 - [7] M.G. Alford and R.L. Jaffe, Nucl. Phys. **B578**, 367 (2000).
 - [8] N. Isgur and H.B. Thacker, Phys. Rev. D **64**, 094507 (2001).
 - [9] T. Schäfer and E.V. Shuryak, hep-lat/0005025.
 - [10] M. Anselmino, E. Predazzi, S. Ekelin, S. Fredriksson, and D.B. Lichtenberg, Rev. Mod. Phys. **65**, 1199 (1993).
 - [11] T. Schäfer, E.V. Shuryak, and J.J. Verbaarschot, Nucl. Phys. **B412**, 143 (1994).
 - [12] R. Rapp, T. Schäfer, E.V. Shuryak, and M. Velkovsky, Phys. Rev. Lett. **81**, 53 (1998).
 - [13] M.G. Alford, K. Rajagopal, and F. Wilczek, Phys. Lett. B **422**, 247 (1998).
 - [14] T. Schäfer and E.V. Shuryak, Rev. Mod. Phys. **70**, 323 (1998).
 - [15] D. Diakonov, Talk given at International School of Physics, “Enrico Fermi,” Varenna, Italy, 1995; hep-ph/9602375.
 - [16] T. DeGrand and A. Hasenfratz, Phys. Rev. D **64**, 034512 (2001).
 - [17] P. Faccioli and T.A. DeGrand, Phys. Rev. Lett. **91**, 182001 (2003).
 - [18] I. Horvath, N. Isgur, J. McCune, and H.B. Thacker, Phys. Rev. D **65**, 014502 (2002); T. DeGrand and A. Hasenfratz, *ibid.* **65**, 014503 (2002); I. Hip, T. Lippert, H. Neff, K. Schilling, and W. Schroers, *ibid.* **65**, 014506 (2002); R.G. Edwards and U.M. Heller, *ibid.* **65**, 014505 (2002); T. Blum *et al.*, *ibid.* **65**, 014504 (2002); C. Gattringer, M. Gockeler, P.E. Rakow, S. Schaefer, and A. Schäfer, Nucl. Phys. **617**, 101 (2001); S.J. Dong *et al.*, Nucl. Phys. B (Proc. Suppl.) **106**, 563 (2002).
 - [19] UKQCD Collaboration, C. Michael, M.S. Foster, and C. Mc-

- Neile, Nucl. Phys. B (Proc. Suppl.) **83**, 185 (2000).
- [20] SCALAR Collaboration, S. Muroya, A. Nakamura, C. Nonaka, M. Sekiguchi, and H. Wada, Nucl. Phys. B (Proc. Suppl.) **106**, 272 (2002).
- [21] RBC Collaboration, S. Prelovsek and K. Orginos, Nucl. Phys. B (Proc. Suppl.) **119**, 822 (2003).
- [22] T. Kunihiro, S. Muroya, A. Nakamura, C. Nonaka, M. Sekiguchi, and H. Wada, hep-ph/0308291.
- [23] R. Gupta, A. Patel, and S.R. Sharpe, Phys. Rev. D **48**, 388 (1993).
- [24] D. Diakonov and V.Y. Petrov, Nucl. Phys. **B272**, 457 (1986).
- [25] M. Kacir, M. Prakash, and I. Zahed, Acta Phys. Pol. B **30**, 287 (1999).
- [26] M. Hutter, Z. Phys. C **74**, 131 (1997).
- [27] T. Schäfer, Phys. Rev. D **66**, 076009 (2002).
- [28] S.R. Cotanch and P. Maris, Phys. Rev. D **66**, 116010 (2002).
- [29] S. Weinberg, Phys. Rev. Lett. **17**, 616 (1966).
- [30] C.W. Bernard, M. Golterman, J. Labrenz, S.R. Sharpe, and A. Ukawa, Nucl. Phys. B (Proc. Suppl.) **34**, 334 (1994).
- [31] C.W. Bernard and M.F. Golterman, Phys. Rev. D **53**, 476 (1996).
- [32] T. Schäfer and E.V. Shuryak, Phys. Rev. D **53**, 6522 (1996); **54**, 1099 (1996).
- [33] E.V. Shuryak and J.J. Verbaarschot, Nucl. Phys. B **410**, 55 (1993).
- [34] M. Lüscher, Commun. Math. Phys. **104**, 177 (1986).
- [35] T. Hatsuda and T. Kunihiro, Phys. Rep. **247**, 221 (1994).
- [36] R. Rapp, T. Schäfer, E.V. Shuryak, and M. Velkovsky, Ann. Phys. (N.Y.) **280**, 35 (2000).
- [37] R.L. Jaffe and F. Wilczek, Phys. Rev. Lett. (to be published).
- [38] R.L. Jaffe, Phys. Rev. Lett. **38**, 195 (1977); **38**, 617(E) (1977).